Pharmaceutical Sciences Asia

Pharm Sci Asia 2026; 53(3), 265-274

DOI:10.29090/psa.2026.03.26.11964

Research Article

Preparation of resveratrol nanocrystals by drug/polymer/surfactant ternary hot extrusion

Thanyaporn Channamom, Shogo Mizuno, Kenjirou Higashi *, Keisuke Ueda, Kunikazu Moribe*

Graduate School of Pharmaceutical Sciences, Chiba University, 1-8-1, Inohana, Chuo-ku, Chiba 260-8675, Japan

ABSTRACT

Drug nanocrystal formulations are an effective strategy for dissolution improvement and oral absorption of poorly water-soluble drugs. In our previous study, we developed a ternary hot extrusion method and demonstrated that drug nanocrystal suspensions can be successfully prepared. In this study, resveratrol (RES) was used as a model poorly water-soluble drug to evaluate the feasibility of this method. A ternary system consisting of RES, polyvinylpyrrolidone K-25 (PVP), and sodium dodecyl sulfate (SDS) was investigated. Physical mixtures (RES/PVP/SDS = 1:3:1 in the weight ratio) were processed using a twin-screw melt mixer to obtain hot extrudates (HE), which were subsequently dispersed in water. Powder X-ray diffraction (PXRD) analysis confirmed that RES remained crystalline in all HE samples. SDS decomposition was observed under high screw speeds (≥250 rpm) and elevated temperatures (130 °C). Cryogenic transmission electron microscopy revealed aggregates of rod-shaped RES nanocrystals (~50 nm) in the HE suspension. PXRD of ultracentrifuged precipitates of HE suspension confirmed that RES retained crystallinity within the nanoparticles. Nanoparticle formation efficiency depended strongly on processing conditions. At 120 °C, higher screw speeds reduced nanoparticle formation due to SDS degradation. At 200 rpm, increasing temperature improved the nanoparticle formation efficiency, reaching a maximum at 125 °C, followed by a decline at 130 °C due to SDS degradation. These results suggest that the optimal conditions for preparing RES nanosuspensions via hot extrusion involve employing relatively high screw rotation speeds and processing temperatures within a range preventing SDS decomposition. This study demonstrates the potential broad applicability of this technique for various poorly water-soluble drugs.

Keywords:
Drug nanocrystal; Hot extrusion; Mechanical force; Heat

1. INTRODUCTION

In recent years, 75–90% of newly developed drug candidates have exhibited poor water solubility, leading to increasing challenges in pharmaceutical formulation development.[1,2] Therefore, improving the solubility of poorly water-soluble drugs through formulation technologies has become essential, and various approaches have been investigated. Drug nanocrystal formulation is one of the most promising approaches for improving drug solubility. Particle size reduction increases the specific surface area, thereby enhancing the dissolution rate.[3,4] In addition, an improvement in drug solubility has been observed, particularly when the particle size is reduced below 100 nm, where the solubility slightly increases compared with coarse particles.[5] Furthermore, drug nanocrystals are expected to improve absorption due to enhanced permeability through the mucin layer near the gastrointestinal mucosa, thereby maintaining a higher drug concentration at the absorption site.[6] Owing to these advantages, several nanocrystal-based formulations have already been marketed.[2]

***Corresponding author:**
* Kenjirou Higashi Email: ken-h@faculty.chiba-u.jp
* Kunikazu Moribe Email: moribe@faculty.chiba-u.jp

Currently, preparation methods for drug nanocrystals include top-down approaches such as dry milling and wet milling as well as bottom-up approaches such as antisolvent precipitation.[7,8] However, existing techniques have limitations related to their principles and equipment configurations. For example, dry milling methods such as ball milling are batch processes, making scale-up difficult and hindering practical application. Wet milling techniques, including bead milling and high-pressure homogenization, are continuous processes suitable for mass production; however, they produce suspensions, which are not suitable for the compounds that easily decompose in water. In addition, a drying process is required to obtain solid dosage forms, and aggregation of drug nanocrystals before and after drying is a major concern. In contrast, bottom-up approaches have difficulty in controlling particle size, and often require organic solvents, the removal of which increases cost and limits practical applications.

Hot melt extrusion has gained attention in the pharmaceutical field, with a significant increase in related patents since the 1980s.[9] In pharmaceutical applications, hot melt extrusion typically involves heating a mixture of drug and thermoplastic excipients over the melting point of drug, kneading it under high shear, and extruding it through a die to obtain a desired shape.[10] This method has been widely used for preparing amorphous solid dispersions where drugs are dispersed in the polymer matrix as amorphous state, and several such formulations have already been commercialized.[11]

Recently we have successfully demonstrated that drug nanosuspensions can be prepared by dispersing a hot extruded ternary mixture of drug, polymer, and surfactant in water, where the mixture is processed at temperatures more than 50 °C below the melting point of drug.[12,13] When extrusion is performed at sufficiently low temperatures relative to the melting point of drug, mechanical shear force from the screw reduces the particle size of drug crystals, and a portion of the drug dissolves into the plasticized polymer (Scheme 1). As a result, a nanodispersion is formed in which drug nanocrystals are dispersed within a polymer matrix. By adding this nanodispersion into water, the surfactant suppresses rapid crystal growth, leading to the formation of a stable drug nanocrystal suspension. However, the investigation thus far is limited, and the applicability of this method to various drugs remains unclear.

In this study, we attempted to prepare drug nanodispersions using the developed ternary hot extrusion method, followed by dispersion in water to obtain drug nanocrystal suspensions. Resveratrol (RES), a poorly water-soluble drug with a high melting point of approximately 267 °C, was selected as a model.[14] Polyvinylpyrrolidone K-25 (PVP) and sodium dodecyl sulfate (SDS), which are commonly used in oral solid dosage forms, were employed as the polymer and surfactant, respectively. First, thermal behavior was evaluated by differential scanning calorimetry (DSC) to determine appropriate extrusion temperatures. Next, the crystallinity of RES in the prepared ternary hot extrudates (HEs) was evaluated by powder X-ray diffraction (PXRD).

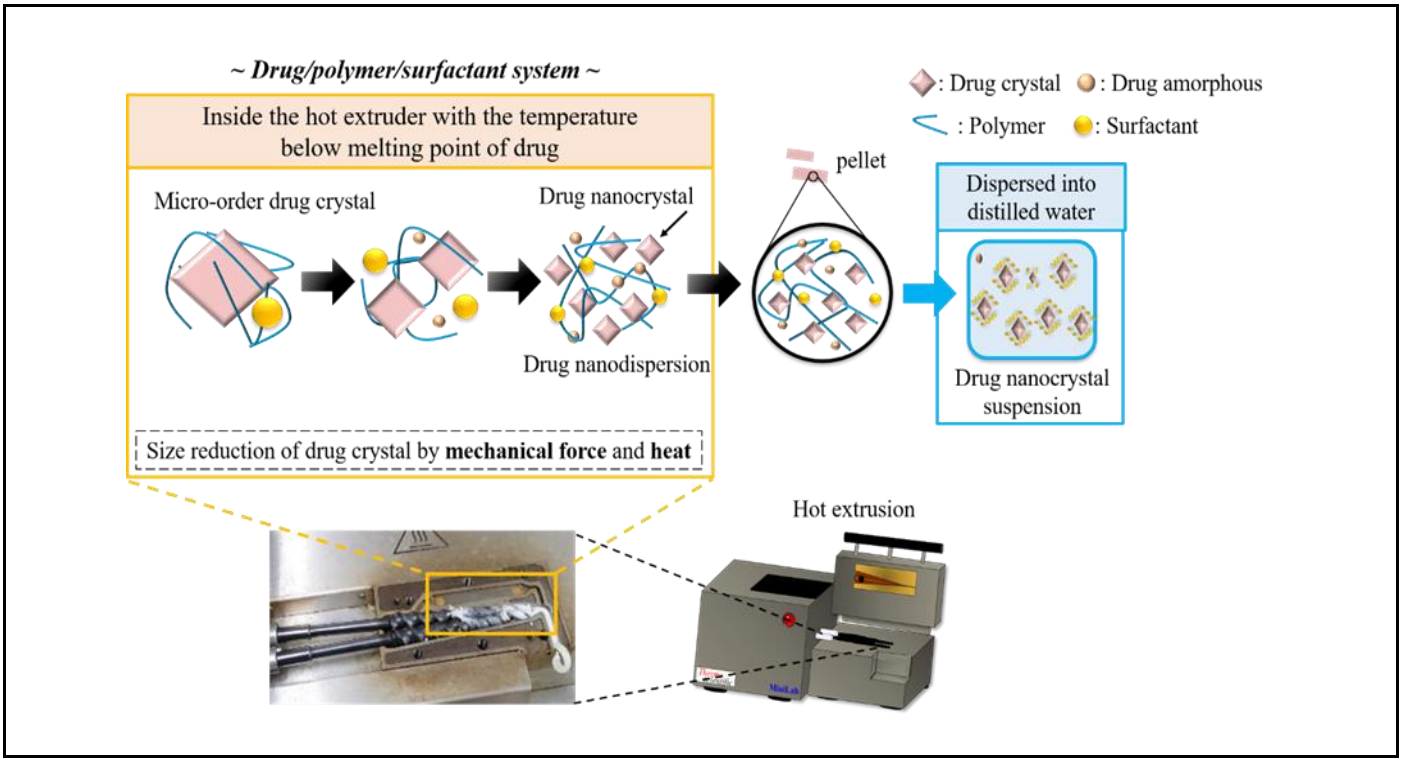

Scheme 1. Schematic illustration of the formation mechanism of drug nanocrystals prepared by hot extrusion.

The suspensions obtained by dispersing the HEs in water were then characterized by particle size analysis, and nanoparticle formation efficiency was determined using the centrifugation method. Furthermore, the morphology of nanoparticles in aqueous dispersion was evaluated by cryogenic transmission electron microscopy (cryo-TEM), and the crystallinity of RES in the precipitate after ultracentrifugation was analyzed by PXRD. Finally, based on these results, the mechanism of RES nanocrystal formation via ternary hot extrusion was discussed.

2. MATERIALS AMD METHODS

2.1. Materials

Resveratrol (RES; Mw 228.24) was purchased from BLD Pharmatech Ltd. (Shanghai, China). Sodium dodecyl sulfate (SDS; Mw 288.38) was obtained from Wako Chemicals Co. (Tokyo, Japan), and sodium sulfate (phase V) was purchased from Nacalai Tesque Inc. (Kyoto, Japan). Polyvinylpyrrolidone K25 (PVP; Mw 25,000–50,000) was kindly provided by BASF Japan Ltd. (Tokyo, Japan). The chemical structures of these compounds are shown in Figure 1.

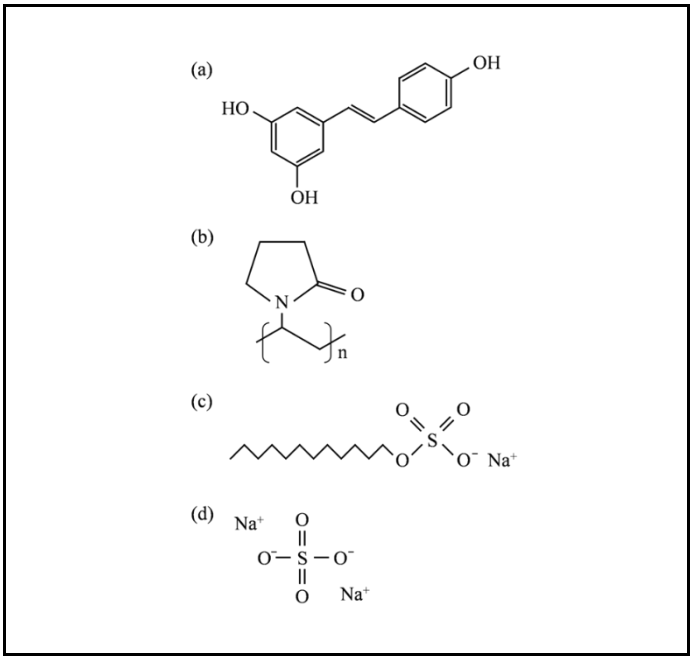

Figure 1. Chemical structures of (a) resveratrol (RES), (b) polyvinylpyrrolidone K-25 (PVP), (c) sodium dodecyl sulfate (SDS), and (d) sodium sulfate (Na_2SO_4).

2.2. Sample preparation

2.2.1. Hot extrudate (HE) and its suspension

Scheme 2 shows the process to prepare HE and its suspension. A physical mixture (PM) was prepared by mixing RES, PVP, and SDS at a mass ratio of 1:3:1 for 5 min using a vortex mixer. Each PM was processed by hot extrusion using a co-rotating twin-screw extruder (HAAKE MiniLab II, Thermo Fisher Scientific Inc., Karlsruhe, Germany) under various conditions, with screw rotation speeds of 150, 200, 250, and 300 rpm and processing temperatures of 110, 115, 120, 125, and 130 °C. The obtained extrudates were cooled at 4 °C for 5 min, then pulverized for 3 min at the frequency of 10/s using a vibration ball mill (MM400, Verder Scientific Co., Ltd., Haan, Germany). The milled samples were then passed through a 100-mesh (150 mm) sieve to obtain the final hot extrudates (HEs). Hereafter, these samples are denoted as HE (screw rotation speed, processing temperature). The HEs were dispersed into distilled water at RES concentration of 1.0 mg/mL, then sonicated for 1 min to prepare HE suspensions.

2.2.2. Na_2SO_4 (phase III) crystal

Sodium sulfate (Na_2SO_4, phase III) was prepared according to the method reported by Bethell et al.[15] Briefly, Na_2SO_4 (phase V) was placed in an aluminum DSC pan. Using a DSC7000X (Hitachi, Tokyo, Japan), the sample was heated to 300 °C at a rate of 20 °C/min under a nitrogen atmosphere (30 mL/min), followed by cooling to 25 °C at the same rate (20 °C/min) to obtain Na_2SO_4 (phase III).

2.3. Analytical methods

2.3.1. Differential scanning calorimetry (DSC)

The samples were placed in aluminum DSC pans and hermetically sealed using lids with a single pinhole to prepare DSC samples. DSC measurements were performed using a DSC7000X (Hitachi, Tokyo, Japan) with a heating rate of 10 °C/min under a nitrogen atmosphere (30 mL/min).

2.3.2. Powder X-ray diffraction (PXRD)

PXRD measurements were carried out using a MiniFlex II (Rigaku Co., Ltd., Tokyo, Japan). The Cu Kα was the radiation source, using a 30 kV acceleration voltage and 15 mA current. Measurements were conducted at a scanning angle of 2θ from 3 to 40º with a scanning speed 1º/min.

2.3.3. Particle size analysis

Particle size distribution was determined by dynamic light scattering at 25 °C using a Zetasizer Ultra (Malvern Panalytical Ltd., Malvern, UK; measurement range: 0.0003–15 μm).

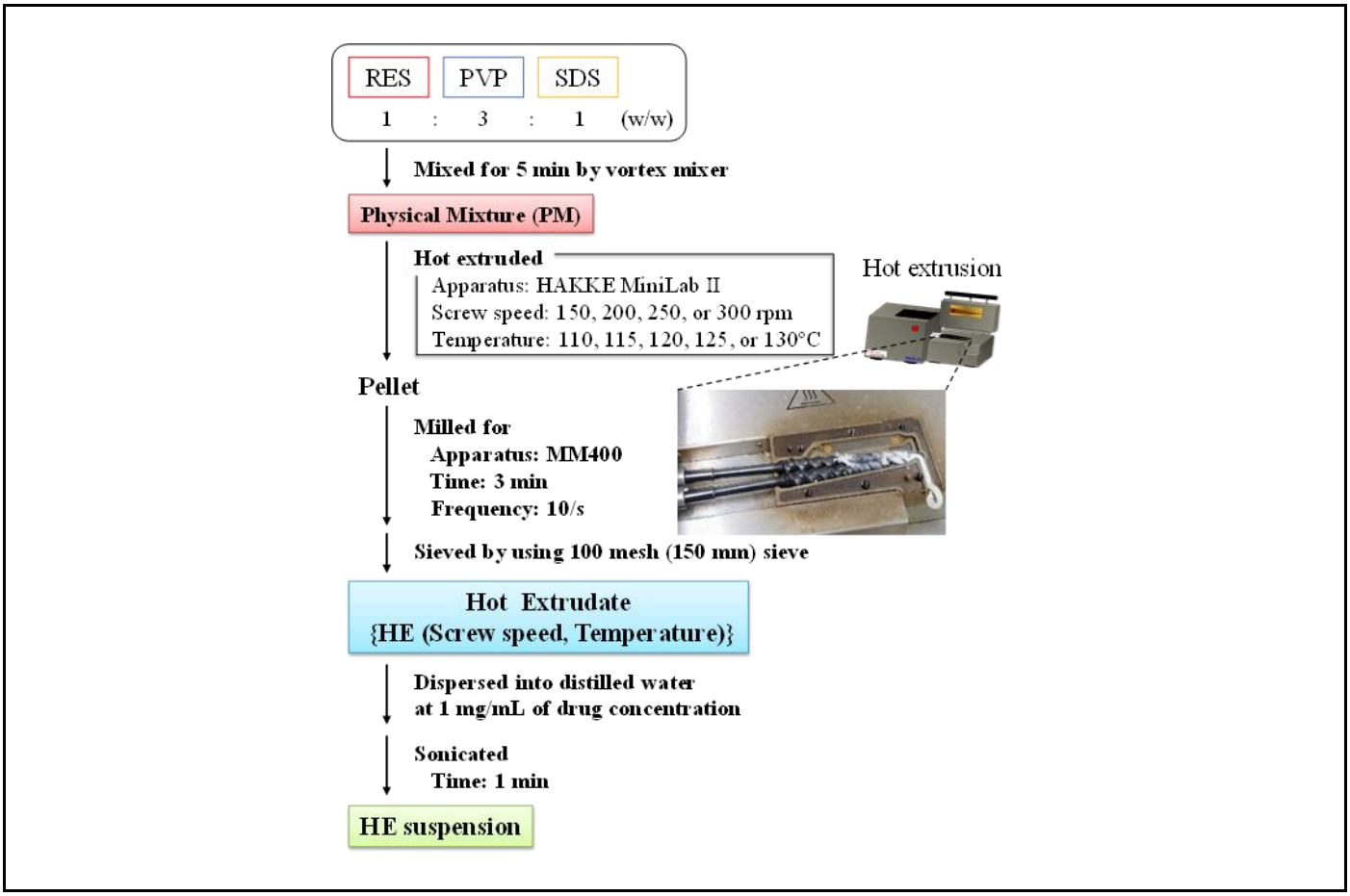

Scheme 2. Preparation method of hot extrudate (HE) and its suspension.

2.3.4. Evaluation of RES nanoparticle formation efficiency

Each suspension was centrifuged at 1,000 ×g at 25 °C for 30 min. The obtained supernatants were appropriately diluted with water/ethanol (1:1, v/v). RES concentration in the diluted samples was determined at a wavelength of 300–350 nm using a UV–visible spectrophotometer (UV-1800, Shimadzu Co., Ltd., Kyoto, Japan). Nanoparticle formation efficiency was discussed from the "recovery rate (%)" of the RES concentration in the supernatant after centrifugation to the total RES concentration in the suspension.

2.3.5. Cryogenic transmission electron microscopy (Cryo-TEM)

Cryo-TEM observations were conducted using a field emission transmission electron microscope (JEM-2100F, JEOL Ltd., Tokyo, Japan) at an acceleration voltage of 120 kV. The support film side of a microgrid (Cu200, Nisshin EM Co., Ltd., Tokyo, Japan) was rendered hydrophilic by treatment with an HDT-400 (JEOL Ltd., Tokyo, Japan) for 60 s. A 3.0 µL aliquot of the sample suspension was then applied onto the grid. Excess liquid was removed with filter paper to form a thin liquid film across the grid holes, and the grid was immediately plunge-frozen in liquid ethane with the temperature control below −170 °C to prepare cryo-TEM specimens. The frozen samples were mounted onto a Gatan 626 cryo-holder (Gatan, Inc., Pleasanton, CA, USA) under liquid nitrogen and observed at temperatures below −170 °C.

3. RESULTS

3.1. Evaluation of HE

3.1.1. DSC

To determine the appropriate processing temperature for preparing a ternary nanodispersion, DSC measurements were conducted. For RES crystal, an endothermic peak corresponding to crystal melting was observed at approximately 270 °C (Figure 2a). For PVP alone, a broad endothermic peak was observed in the range of 40–130 °C, which was attributed to dehydration (Figure 2b). According to Maria et al., the glass transition temperature (T_g) of PVP stored under 54% relative humidity is 50.3 °C.[16] Since the PVP used in this study was not subjected to a dehydration process, it was assumed to have a similar T_g. In the present measurement, no baseline shift attributable to the T_g of

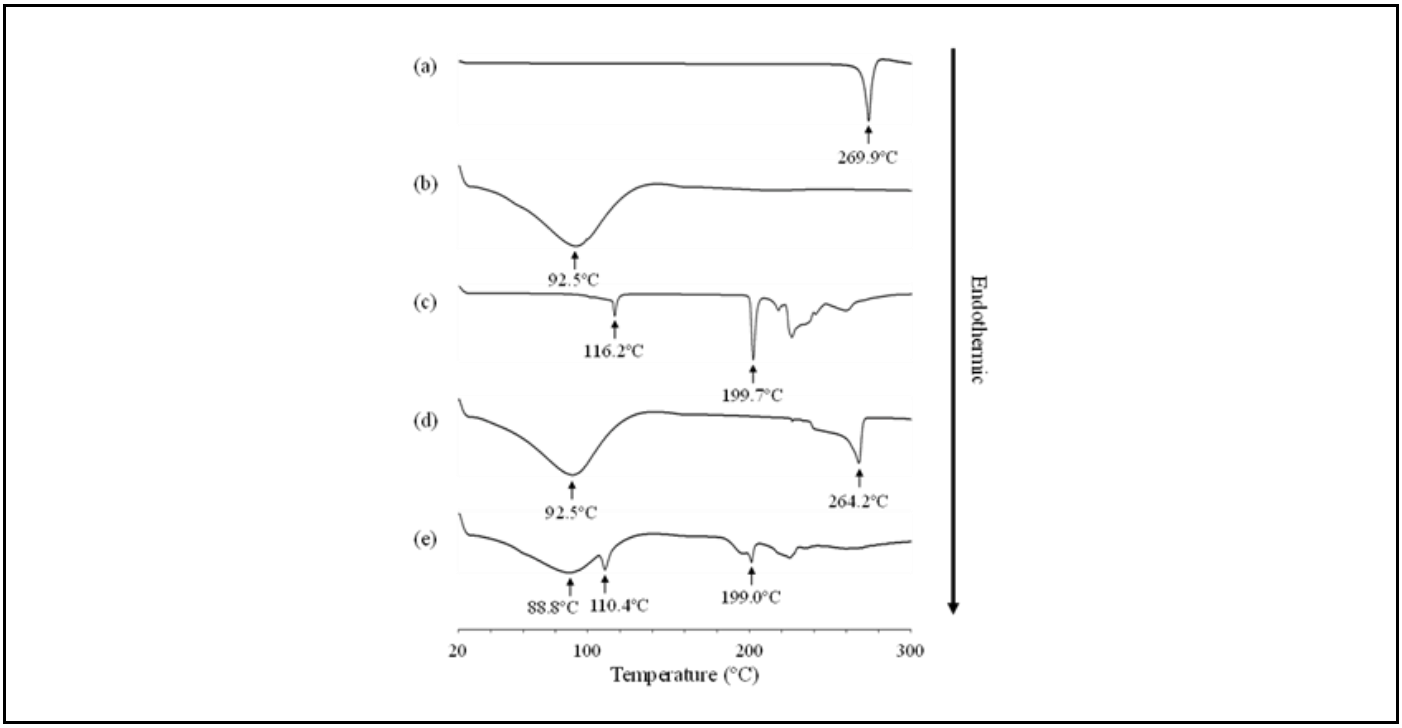

Figure 2. Differential scanning calorimetry (DSC) profiles of (a) RES, (b) PVP, (c) SDS, (d) RES/PVP PM, and (e) RES/PVP/SDS PM.

PVP was observed because it was masked by the dehydration peak. For SDS alone, an endothermic peak due to dehydration was observed at 116.2 °C, along with a melting peak around 200 °C and peaks above 220 °C, suggesting thermal decomposition[17] (Figure 2c). In the RES/PVP PM, both the melting peak of RES and the dehydration peak of PVP were observed (Figure 2d). In contrast, the RES/PVP/SDS PM exhibited not only the broad dehydration peak of PVP (88.8 °C) but also the dehydration peak of SDS (110.4 °C) (Figure 2e). Multiple endothermic peaks were observed above 180 °C, which were probably attributed to the melting and/or decomposition of RES and SDS; however, precise assignment was difficult. Based on these results, since no melting peak of RES was observed below 180 °C and SDS thermal decomposition occurred above 220 °C, a processing temperature of approximately 120 °C was selected. This temperature is sufficiently lower than these critical temperatures while being above the T_g of PVP.

3.1.2. PXRD

PXRD measurements were conducted to evaluate the crystallinity of RES in each HE (Figure 3).

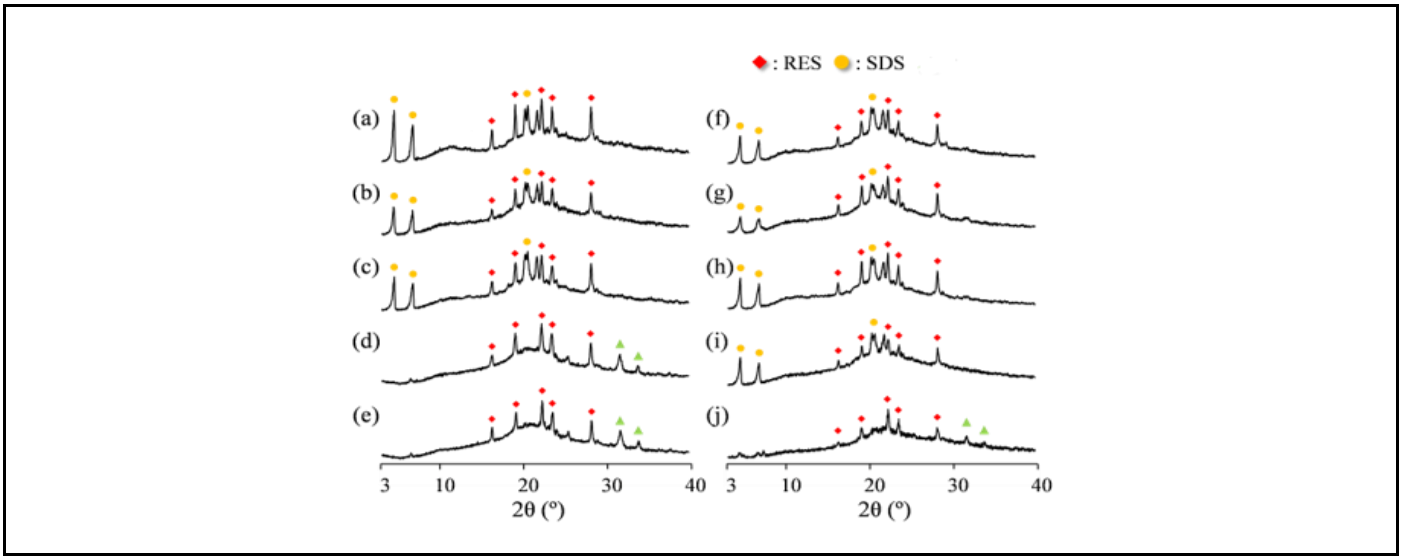

Figure 3. Powder X-ray diffraction (PXRD) patterns of (a) RES/PVP/SDS PM, (b) HE (150, 120), (c) HE (200, 120), (d) HE (250, 120), (e) (300, 120), (f) HE (200, 110), (g) HE (200, 115), (h) HE (200, 120), (i) HE (200, 125), and (j) HE (200, 130).

For the HE samples prepared at a fixed processing temperature of 120 °C with varying screw rotation speeds (HE (150–300, 120)), diffraction peaks attributable to RES crystal (as shown in red diamond) were observed in all samples, indicating the presence of crystalline RES. On the other hand, in the HE samples processed at relatively high screw rotation speeds (HE (250–300, 120)), the intensity of characteristic diffraction peaks of SDS at 2θ = 4.5° and 6.7° (as shown in yellow circle) decreased, while additional peaks (as shown in green triangle) appeared at 2θ = 31.8° and 34.0°, suggesting the decomposition of SDS. Since the thermal decomposition of SDS is known to occur above 180 °C[17], these results indicate that factors other than temperature contributed to the decomposition. It is considered that the increased shear force associated with higher screw rotation speeds introduced excessive energy into the sample, leading to SDS decomposition. For HE samples prepared at a fixed screw rotation speed of 200 rpm with varying temperatures (HE (200, 110–130)), crystalline RES was detected in all samples. No SDS decomposition was observed in HE prepared at lower temperatures 110–125 ℃. However, SDS decomposition was observed in HE prepared at 130℃, suggesting that excessive temperature elevation can also induce SDS decomposition.

To identify the decomposition products of SDS, the PXRD pattern of HE (200, 130) was compared with those of possible decomposition products (Figure 4). The diffraction peaks at 2θ = 31.8° and 34.0°, attributed to decomposition products in HE (200, 130), were found to be consistent with the pattern of sodium sulfate (Na_2SO_4) in its metastable phase III.[18] SDS has been reported to undergo hydrolysis in aqueous environments to form 1-dodecanol and sulfuric acid.[15,19] In the present study, although the reaction occurred in the solid state, it is inferred that SDS underwent hydrolysis to produce 1-dodecanol and Na_2SO_4. It is possible that moisture absorbed by PVP served as the water source for this reaction.

3.2. Evaluation of HE suspensions

3.2.1. Nanoparticle formation efficiency

To determine the proportion of drug nanoparticles contained in the HE samples, each HE suspension was subjected to centrifugation, and the ratio of the RES concentration in the supernatant after centrifugation to the total RES concentration in the HE suspension was calculated as the recovery rate.[20,21] Based on particle size distribution measurements of the supernatant obtained from HE (200, 125) after centrifugation, it was confirmed that relatively larger particles sedimented during centrifugation, while particles with an average size of approximately 180 nm remained in the supernatant (Figure 5). Therefore, the recovery rate represents the proportion of RES in the suspension that is present in the bulk water phase as dissolved state and/or in the nanoparticles approximately 180 nm as crystalline state.

Figure 6 shows the recovery rate of PM suspension and each HE suspension. For HE samples processed at 120 °C (HE (150–300, 120)), the recovery rate decreased at higher screw rotation speeds (HE (250–300, 120)). This was attributed to the decomposition of SDS, as confirmed by the PXRD results shown in Figure 3. For HE samples prepared at a fixed screw rotation speed of 200 rpm (HE (200, 110–130)), an increasing trend in recovery rate was observed with increasing processing temperature, reaching a maximum value of 65% at 125 °C. However, at 130 °C,

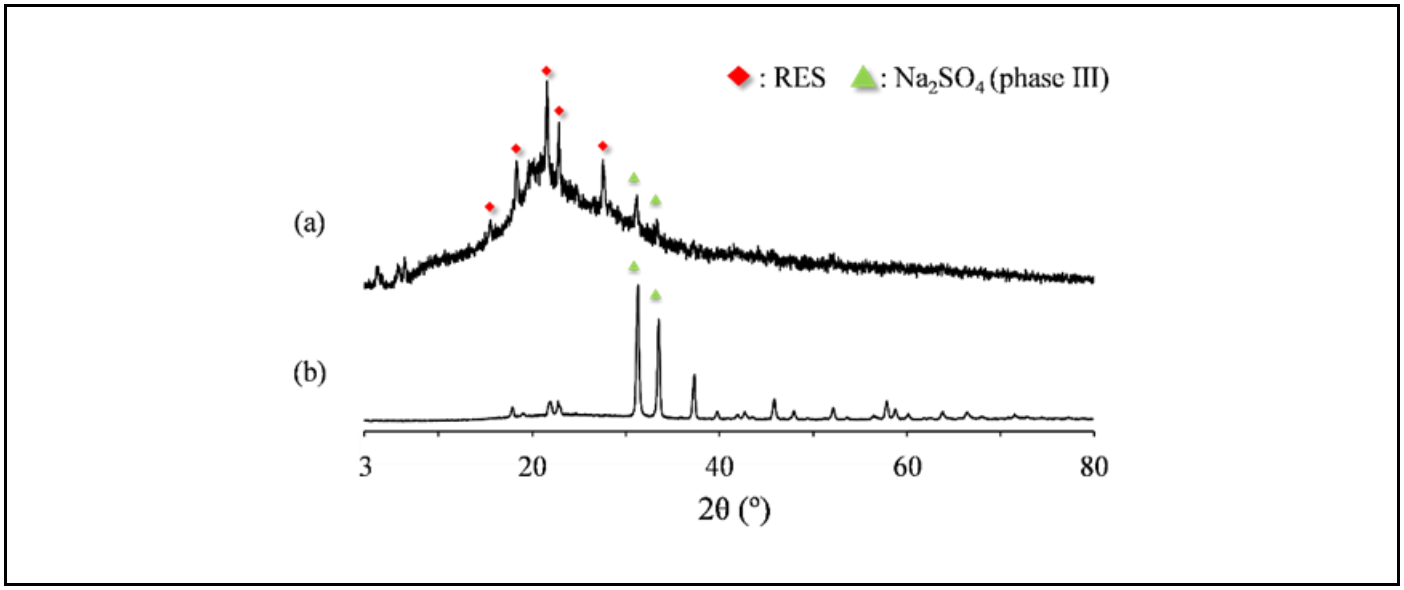

Figure 4. PXRD patterns of (a) HE (200, 130) and (b) Na_2SO_4 (phase III).

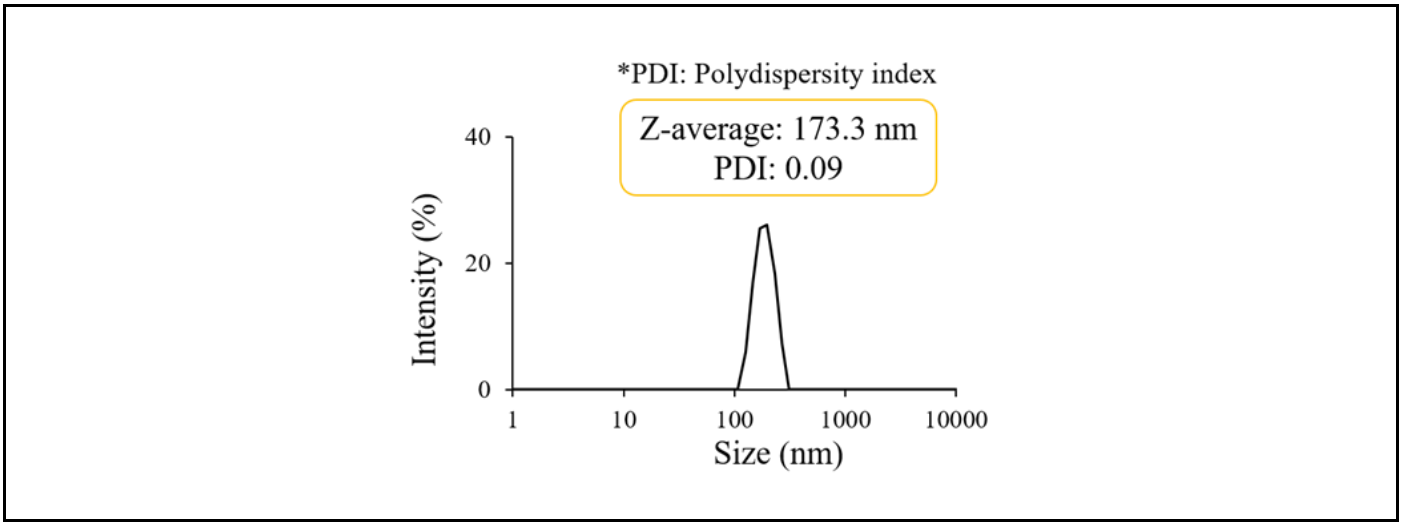

Figure 5. Particle size distributions of HE (200, 125) suspensions after centrifugation at 1,000 ×g at 25 °C for 30 min.

the recovery rate decreased. Since SDS decomposition was also confirmed in this sample (Figure 3), this decrease was attributed to the same effect.

3.2.2. PXRD and Cryo-TEM

To evaluate the crystallinity of RES in the HE suspension, HE (200, 125) was subjected to ultracentrifugation, and the precipitate was collected and dried under reduced pressure for PXRD analysis (Figure 7a). Only diffraction peaks corresponding to crystalline RES were observed, indicating that the majority of the precipitate consisted of crystalline RES. In addition, cryo-TEM observations of the HE (200, 125) suspension revealed that, after dispersion in water, RES formed primary rod-shaped crystals with a size of approximately 50 nm, which further aggregated to form larger structures (Figure 7b). The anionic surfactant SDS is presumed to adsorb onto the surface of RES nanocrystals, orienting its hydrophobic alkyl chain toward

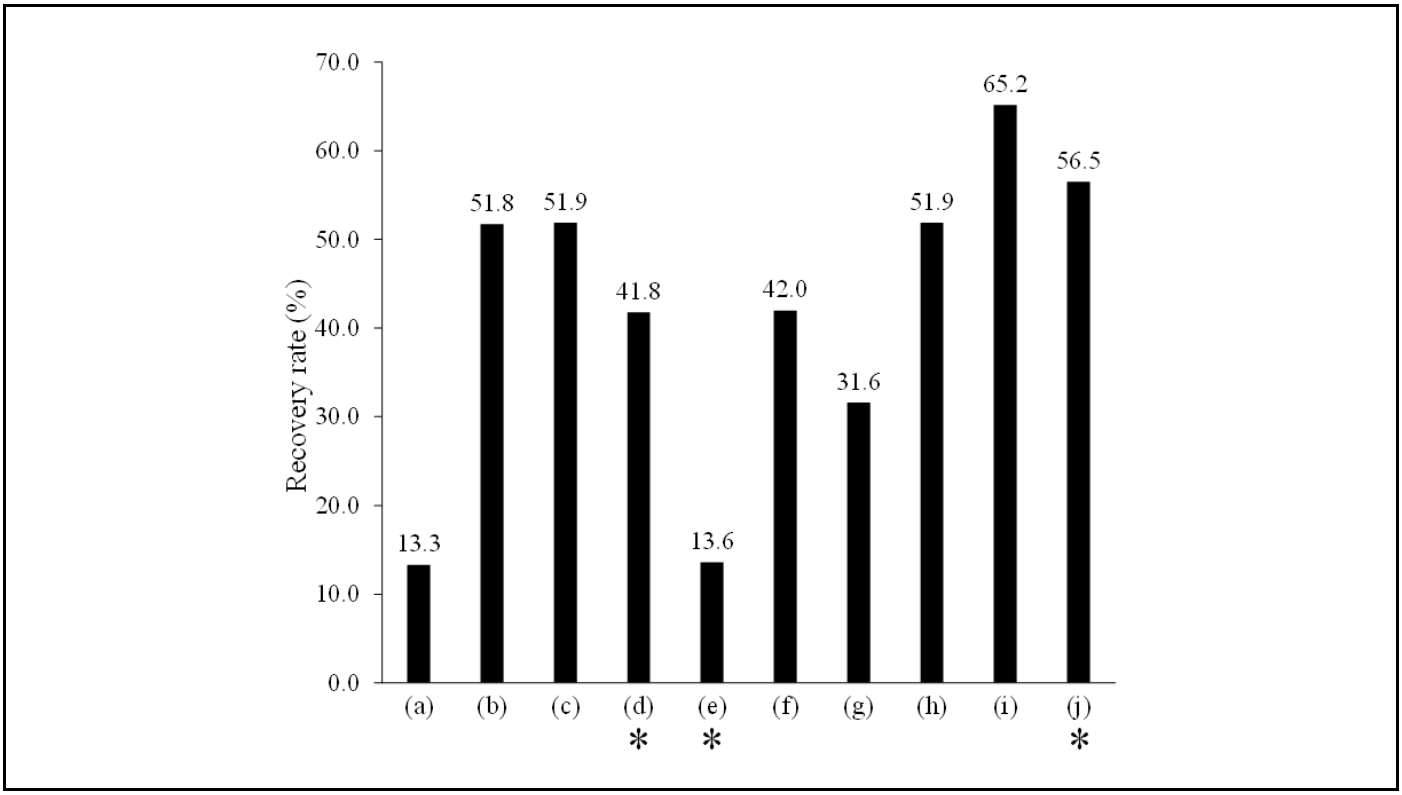

Figure 6. Recovery rates of each suspension: (a) RES/PVP/SDS PM, (b) HE (150, 120), (c) HE (200, 120), (d) HE (250, 120), (e) HE (300, 120), (f) HE (200, 110), (g) HE (200, 115), (h) HE (200, 120), (i) HE (200, 125), and (j) HE (200, 130). In the samples of (d), (e), and (j), which were represented by asterisks, SDS decomposition was observed in Figure 3.

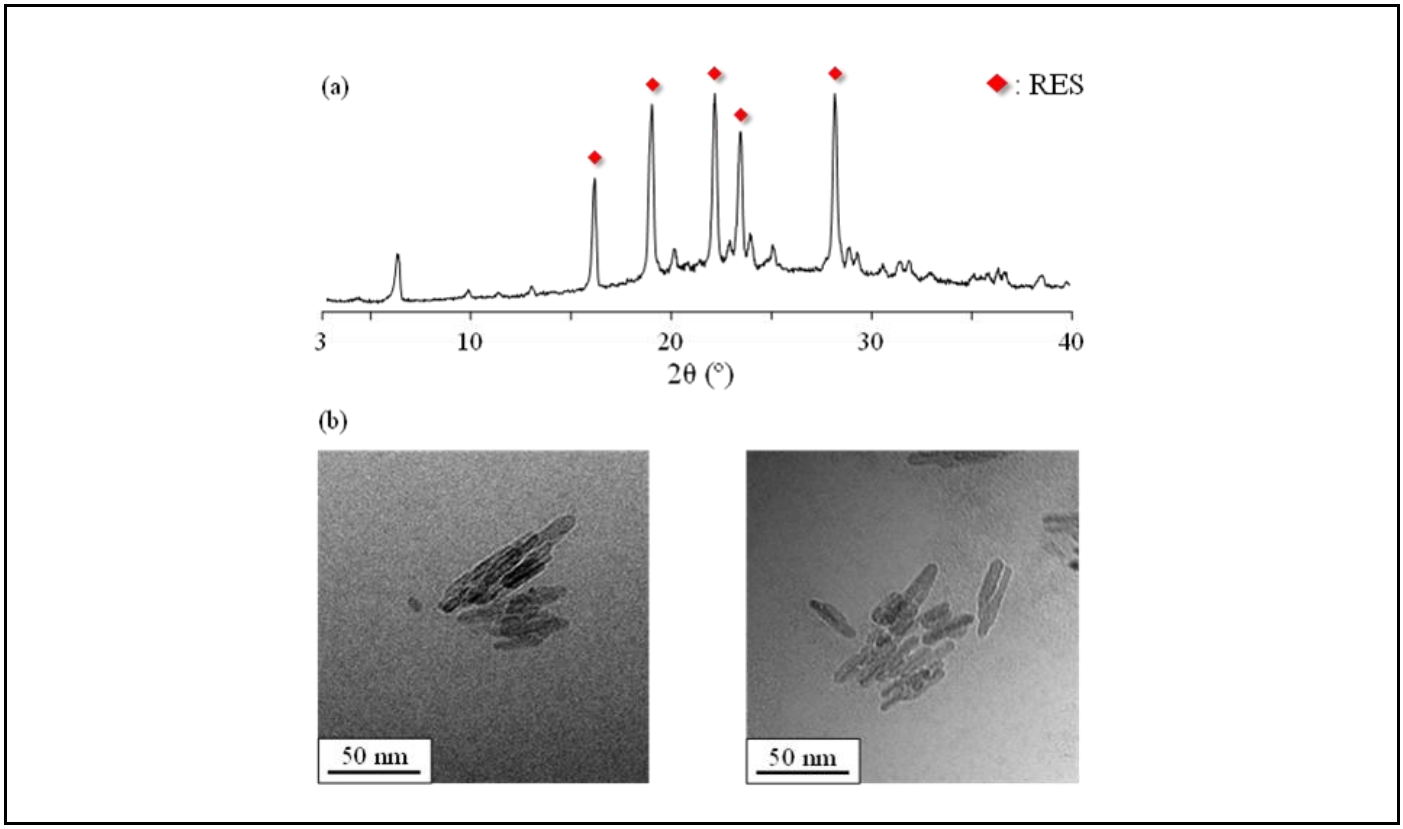

Figure 7. (a) PXRD pattern of dried precipitate of ultracentrifugated HE (200, 125) suspension, and (b) cryo-TEM images of HE (200, 125) suspension.

the RES crystal and its hydrophilic sulfate group toward the aqueous phase.[22] The electrostatic repulsion arising from the negatively charged sulfate groups of SDS prevents aggregation of the RES nanocrystals. Although some aggregated structures were observed in the present nanosuspension, it is considered that SDS adsorption effectively suppressed further aggregation of RES nanocrystals in water, resulting in a high recovery rate.

4. DISCUSSION

Figure 8 summarizes the effects of various hot extrusion conditions on the physical state of the RES in the HE samples and on the colloidal RES nanocrystals after aqueous dispersion. For all HE samples prepared at a processing temperature of 120 °C (HE (150–300, 120)), the presence of crystalline RES was confirmed (Figure 3). When the screw rotation speed was 200 rpm or lower, no decomposition of SDS was observed, whereas SDS decomposition occurred at screw speeds of 250 rpm or higher. In HE samples where SDS remained intact after processing (HE (150–200, 120)), aggregation of RES nanocrystals during aqueous dispersion was effectively suppressed by SDS, resulting in relatively high recovery rate. In contrast, for HE samples in which SDS had decomposed (HE (250–300, 120)), aggregation of nanoparticles during dispersion could not be sufficiently prevented, leading to a decrease in recovery rate. Next, for HE samples prepared at a fixed screw rotation speed of 200 rpm with varying processing temperatures (HE (200, 110–130)), the recovery rate increased with increasing temperature, reaching a maximum value of 65% at 125 °C. The increase in temperature promotes PVP plasticization, allowing a larger amount of RES to dissolve into the PVP matrix, thereby reducing the size of RES nanocrystals in the HE.[12,13] As a result, higher processing temperatures led to the formation of a large amount of RES nanocrystals upon aqueous dispersion. However, when the processing temperature exceeded 130 °C, the thermal energy applied to the samples became excessive, leading to the decomposition of SDS. Consequently, aggregation of nanoparticles during aqueous dispersion could not be sufficiently suppressed, resulting in a decrease in recovery rate. These findings suggest that optimization of both processing temperature and screw rotation speed is critical for achieving improved drug dispersion in polymer matrix and efficient nanoparticle formation in water.

5. CONCLUSION

It was demonstrated that RES colloidal nanocrystals can be successfully prepared via ternary hot extrusion of RES/PVP/SDS. Furthermore, it was found that the nanoparticle formation efficiency of RES

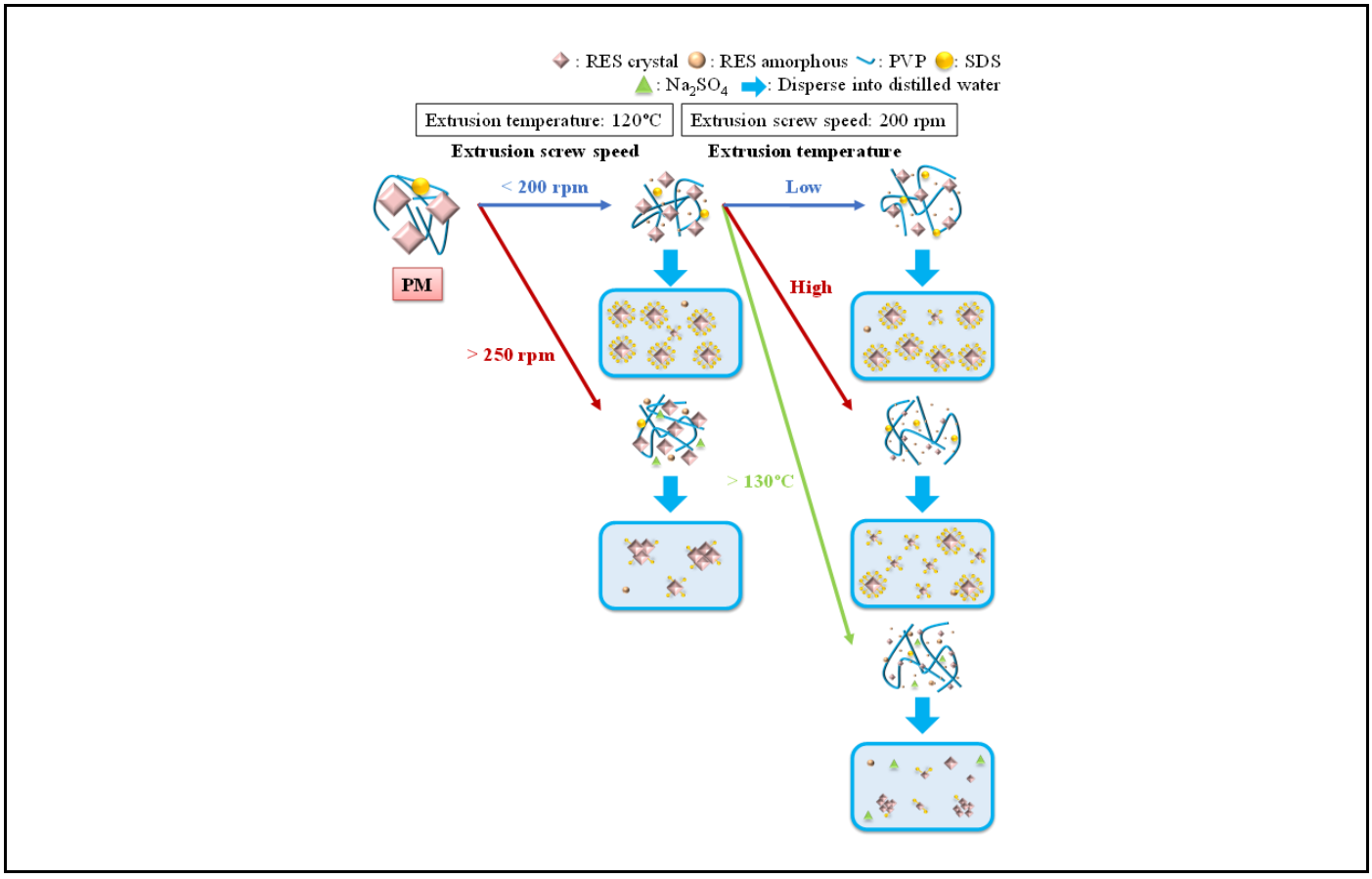

Figure 8. Speculated mechanism of RES nanoparticle formation from HEs.

varied depending on the processing conditions. At higher screw rotation speeds or processing temperatures, SDS was shown to decompose, resulting in the formation of Na_2SO_4 (phase III). The reduction in SDS content led to insufficient suppression of nanoparticle aggregation during aqueous dispersion, thereby decreasing the RES nanoparticle formation efficiency. Accordingly, the optimal conditions for preparing RES nanocrystalline suspensions via hot extrusion involve employing relatively high screw rotation speeds and processing temperatures within a range that prevents SDS decomposition. This method takes advantage of the unique characteristics of hot extrusion and overcomes several limitations of conventional drug nanocrystal preparation techniques. The findings of this study are expected to provide valuable insights for the design and development of various drug nanocrystal formulations.

6. ACKNOWLEDGMENT

We would like to acknowledge BASF Japan Ltd. for kindly providing PVP.

Author contributions

Thanyaporn Channamom: Conceptualization, Methodology, Writing-original draft. Shogo Mizuno: Conceptualization, Methodology, Writing-original draft. Kenjirou Higashi: Conceptualization, Methodology, Writing-review & editing, Funding acquisition, Supervision. Keisuke Ueda: Conceptualization, Methodology, Writing-review & editing. Kunikazu Moribe: Conceptualization, Methodology, Writing-review & editing, Funding acquisition, Supervision.

Funding

This work was supported by a research grant from the Research Grant from the Urakami Foundation for Food and Food Culture Promotion.

Conflict of interest

The authors have no conflicts of interest to disclose.

Ethical approval

None to declare

Article info:

Received June 25, 2026
Received in revised form August 14, 2026
Accepted August 16, 2026

REFERENCES

1. Bennett-Lenane H, O'Shea JP, O'Driscoll CM, Griffin BT. A retrospective biopharmaceutical analysis of >800 approved

oral drug products: Are drug properties of solid dispersions and lipid-based formulations distinctive?. J Pharm Sci. 2020;109(11):3248–61.
2. Ueda K, Porter CJH, Goodwin A, Taylor LS. The expanding role of formulations to enable oral delivery of poorly water-soluble drugs. Nat. Rev. Drug Discov. 2026;25(7):553-75.
3. Mauludin R, Müller RH, Keck CM. Development of an oral rutin nanocrystal formulation. Int J Pharm. 2009;370(1–2):202–9.
4. Brough C, Williams RO. Amorphous solid dispersions and nano-crystal technologies for poorly water-soluble drug delivery. Int J Pharm. 2013;453(1):157–66.
5. Eerdenbrugh BV, Vermant J, Martens JA, Froyen L, Humbeeck JV, Van G, et al. Solubility increases associated with crystalline drug nanoparticles: Methodologies and significance. Mol Pharm. 2010;7(5):1858–70.
6. Roos C, Dahlgren D, Sjögren E, Sjöblom M, Hedeland M, Lennernäs H. Jejunal absorption of aprepitant from nanosuspensions: Role of particle size, prandial state and mucus layer. Eur J Pharm Biopharm. 2018;132:222–30.
7. Malamatari M, Taylor KMG, Malamataris S, Douroumis D, Kachrimanis K. Pharmaceutical nanocrystals: Production by wet milling and applications. Drug Discov Today. 2018;23(3):534–47.
8. Al-Kassas R, Bansal M, Shaw J. Nanosizing techniques for improving bioavailability of drugs. J Control Release. 2017;260:202–12.
9. Simões MF, Pinto RMA, Simões S. Hot-melt extrusion in the pharmaceutical industry: Toward filing a new drug application. Drug Discov Today. 2019;24(9):1749–68.
10. Patil H, Vemula SK, Narala S, Lakkala P, Munnangi SR, Narala N, et al. Hot-melt extrusion: From theory to application in pharmaceutical formulation—Where are we now?. AAPS PharmSciTech. 2024;25(2).
11. Alzahrani A, Nyavanandi D, Mandati P, Youssef AAA, Narala S, Bandari S, et al. A systematic and robust assessment of hot-melt extrusion-based amorphous solid dispersions: Theoretical prediction to practical implementation. Int J Pharm. 2022;624:121951.
12. Omagari K, Ueda K, Zhijing Z, Higashi K, Inoue M, Fukami T, et al. Mechanistic study of preparation of drug/polymer/surfactant ternary hot extrudates to obtain small and stable drug nanocrystal suspensions. Int J Pharm. 2020;591:120003.
13. Hanada N, Higashi K, Zhao Z, Ueda K, Moribe K. Preparation of a ternary amorphous solid dispersion using hot-melt extrusion for obtaining a stable colloidal dispersion of amorphous probucol nanoparticles. Int J Pharm. 2023;640:122959.
14. Zhou H, Wang Y, Li S, Lu M. Improving chemical stability of resveratrol in hot melt extrusion based on formation of eutectic with nicotinamide. Int J Pharm. 2021;607:121042–2.
15. Bethell D, Fessey RE, Namwindwa E, Roberts DW. The hydrolysis of C12 primary alkyl sulfates in concentrated aqueous solutions. Part 1. general features, kinetic form and mode of catalysis in sodium dodecyl sulfate hydrolysis†. J Chem Soc Perkin Trans. 2. 2001;(9):1489–95.
16. Doreth M, Löbmann K, Priemel P, Grohganz H, Taylor R, Holm R, et al. Influence of PVP molecular weight on the microwave assisted in situ amorphization of indomethacin. Eur J Pharm Biopharm. 2018;122:62–9.
17. Lee T, Yeh KL, You JX, Fan YC, Cheng YS, Pratama DE. Reproducible crystallization of sodium dodecyl sulfate·1/8 hydrate by evaporation, antisolvent addition, and cooling. ACS Omega. 2020;5(2):1068–79.
18. Proydakova VYu, Voronov VV, Pynenkov AA, Kuznetsov SV, Zykova MP, Nishchev KN, et al. Sodium sulfate polymorphism. Russ J Inorg Chem. 2022;67(7):970–7.
19. Nakagaki M, Yokoyama S. Acid-catalyzed hydrolysis of sodium dodecyl sulfate. J Pharm Sci. 1985;74(10):1047–52.
20. Wongmekiat A, Tozuka Y, Moribe K, Oguchi T, Yamamoto K. Preparation of drug nanoparticles by co-grinding with cyclodextrin: Formation mechanism and factors affecting nanoparticle formation. Chem Pharm Bull. 2007;55(3):359–63.
21. Gupta VK, Patel JP. A one-parameter model for describing the residence time distribution of closed continuous flow systems characterized by nonlinear reaction kinetics: Rod and ball mills. Powder Tech. 2015;274:163–72.
22. Zhao Z, Katai H, Higashi K, Ueda K, Kawakami K, Moribe K. Cryo-TEM and AFM observation of the time-dependent evolution of amorphous probucol nanoparticles formed by the aqueous dispersion of ternary solid dispersions. Mol Pharm. 2019;16(5):2184–98.